Roles of basicity and steric crowding of anionic coligands in catechol oxidase like activity of Cu(II)-Mn(II) Complexes.

Sabarni Dutta[a], Pradip Bhunia[a], Júlia Mayans[b], Michael G. B. Drew[c], Ashutosh Ghosh[a,*]

[a]Department of Chemistry, University College of Science, University of Calcutta, 92, A.P.C. Road, Kolkata 700 009, India, E-mail address: ghosh_59@yahoo.com

[b]Departament de Química Inorgànica I Orgànica, Secció Inorgànica and Institut de Nanosciència I Nanotecnologia (IN^{2}UB). Martíi Franqués 1-11. 08028, Barcelona, Spain.

[c]School of Chemistry, The University of Reading, P.O. Box 224, Whiteknights, Reading RG6 6AD, UK.

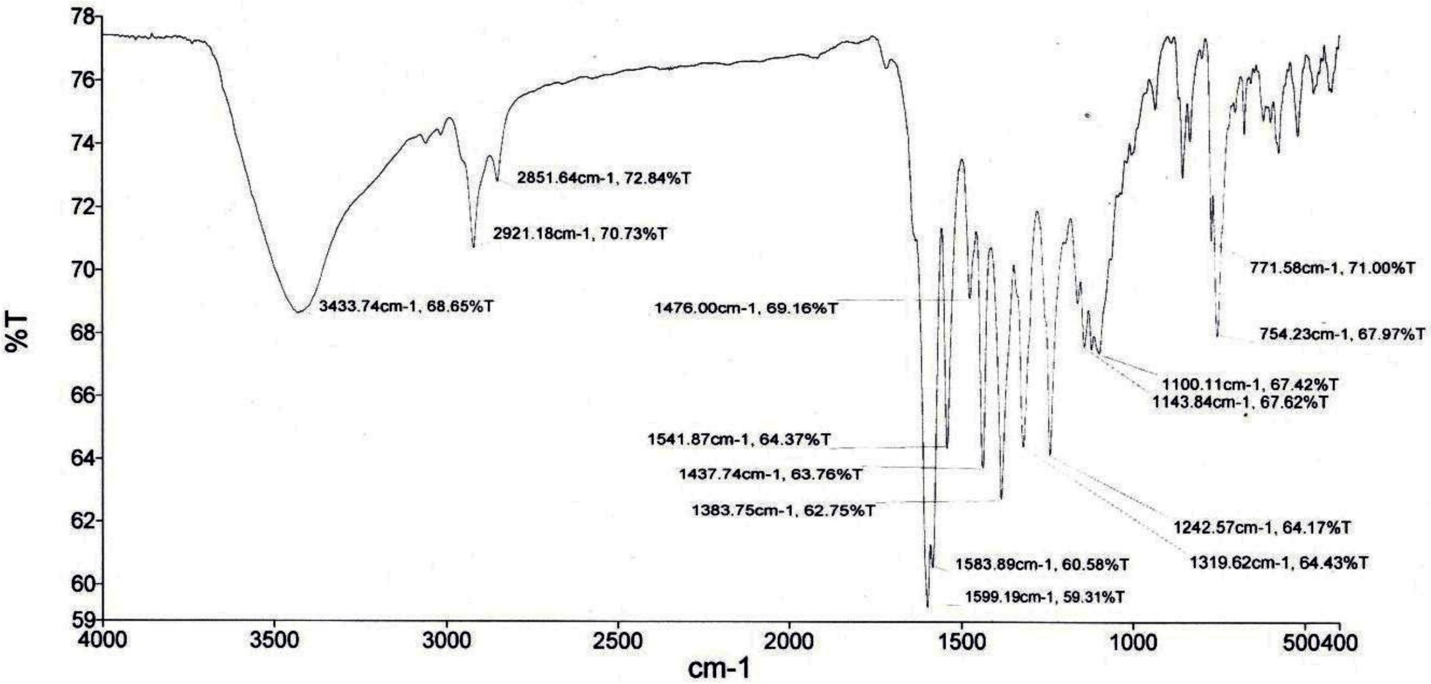

Fig. S1. Representative IR spectrum of Complex **1**.

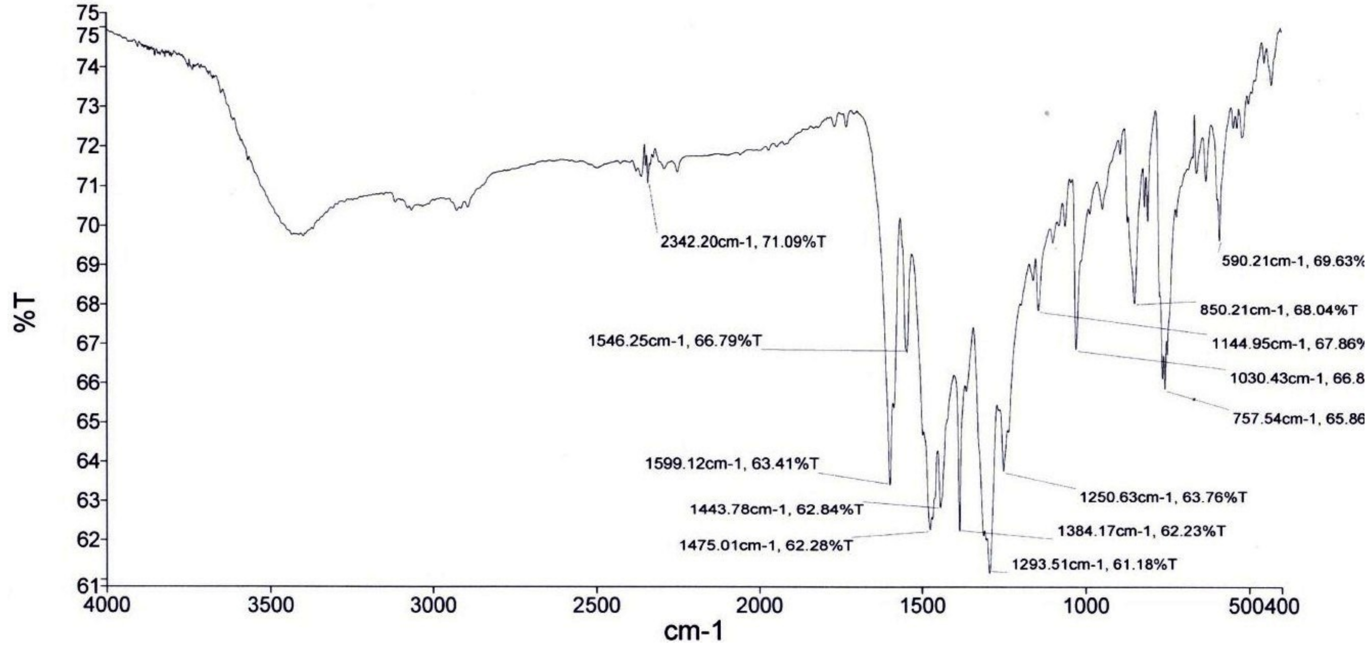

Fig. S2. Representative IR spectrum of Complex **2**.

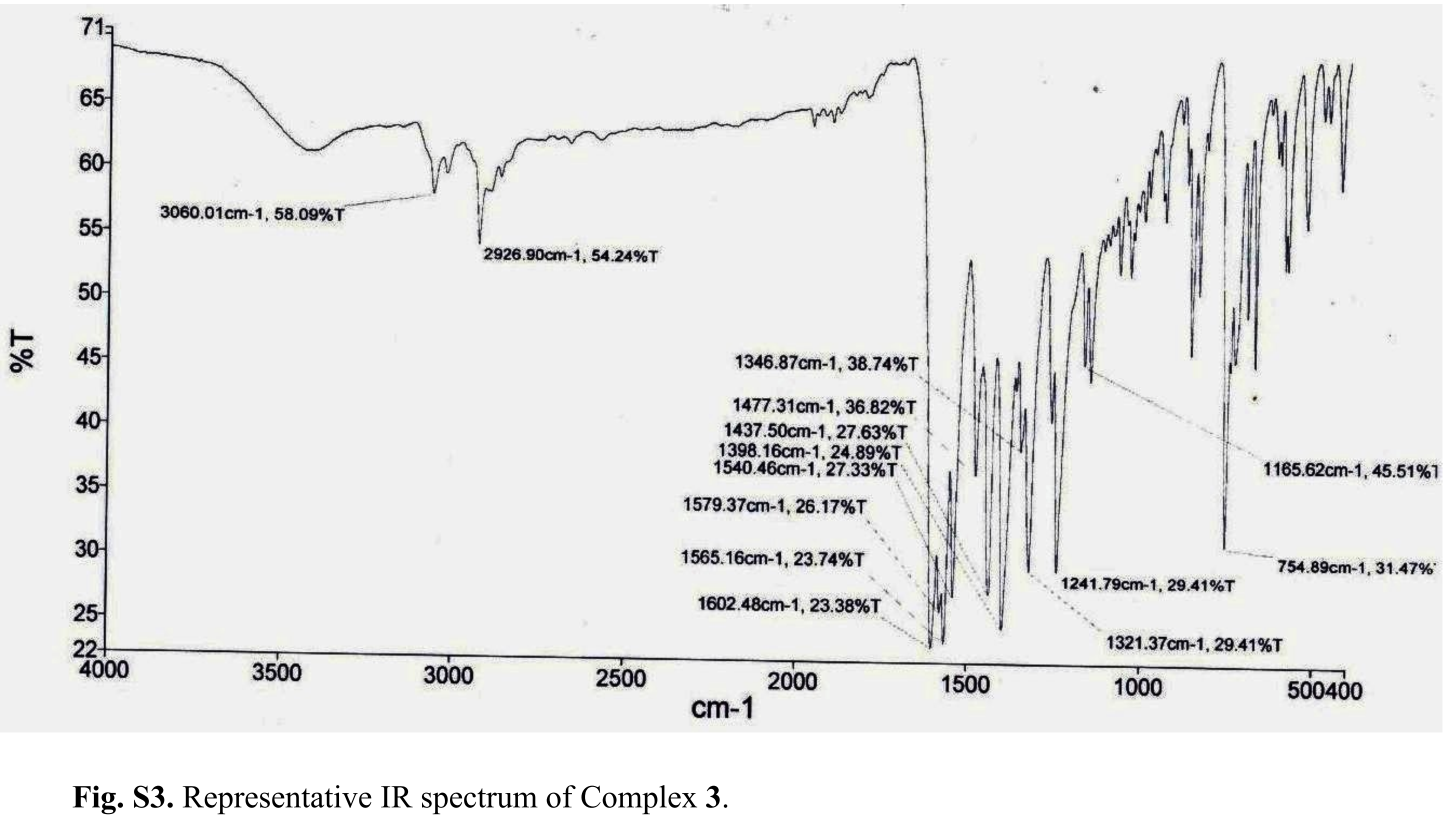

Fig. S3. Representative IR spectrum of Complex **3**.

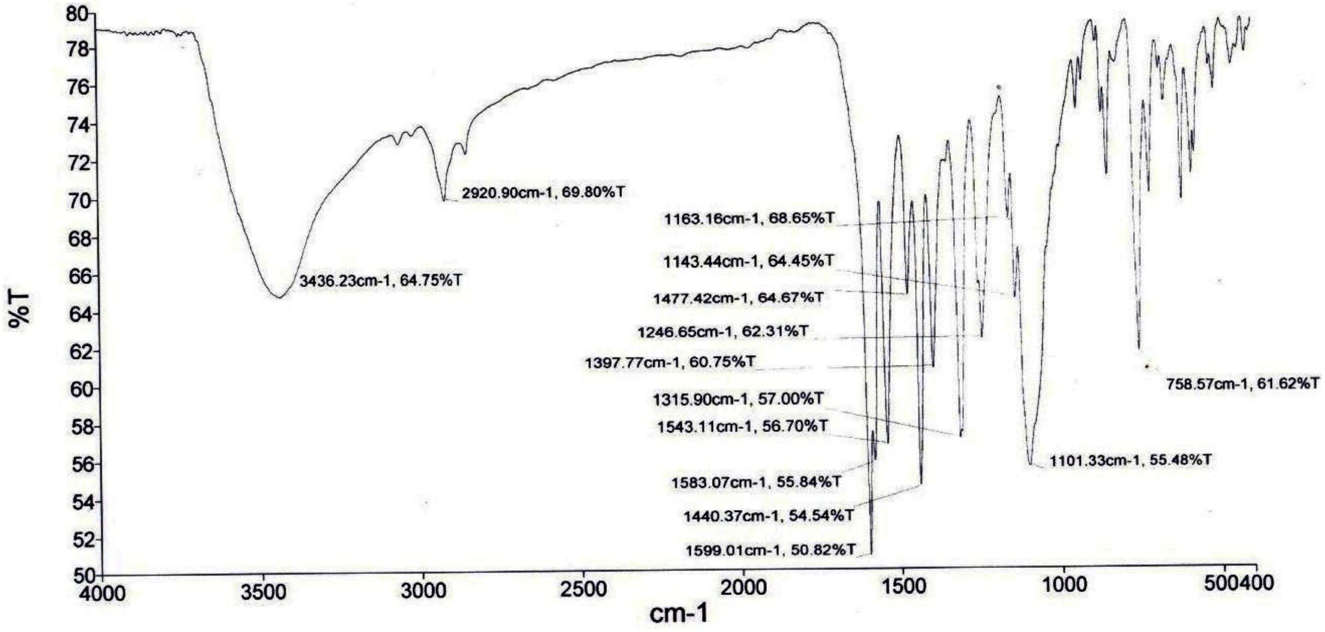

Fig. S4. Representative IR spectrum of Complex **4**.

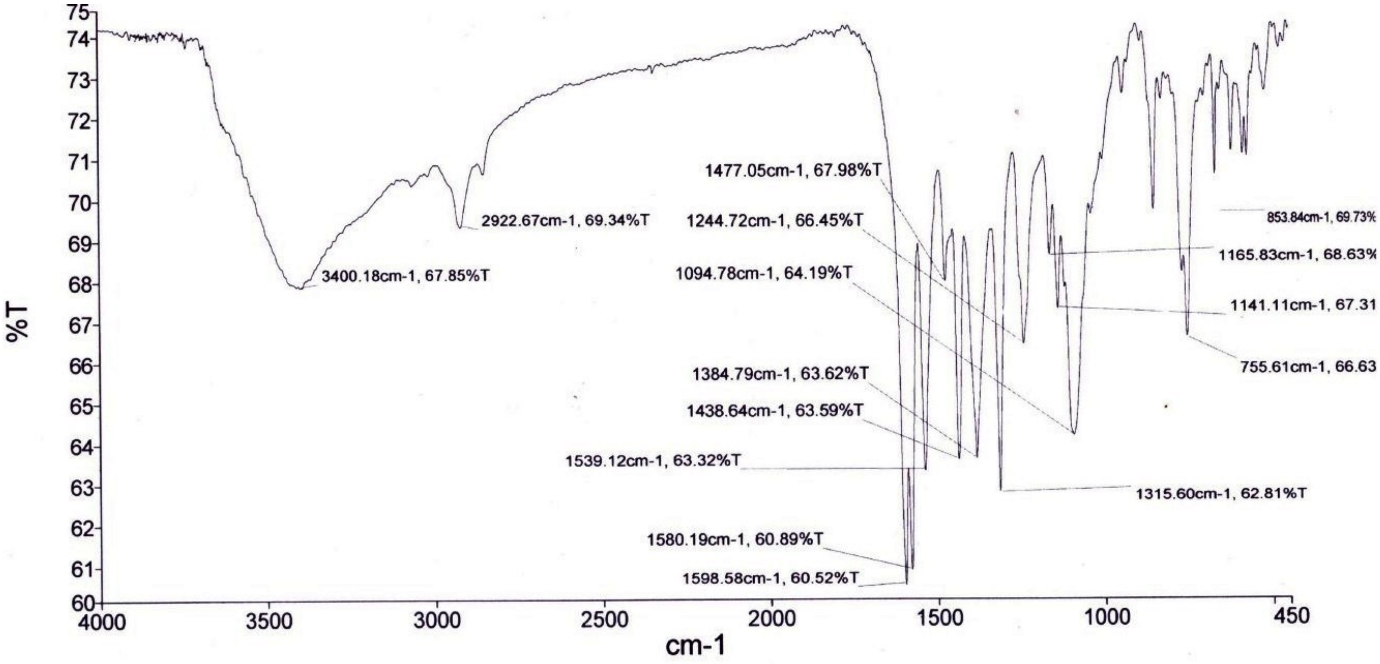

Fig. S5. Representative IR spectrum of Complex **5**.

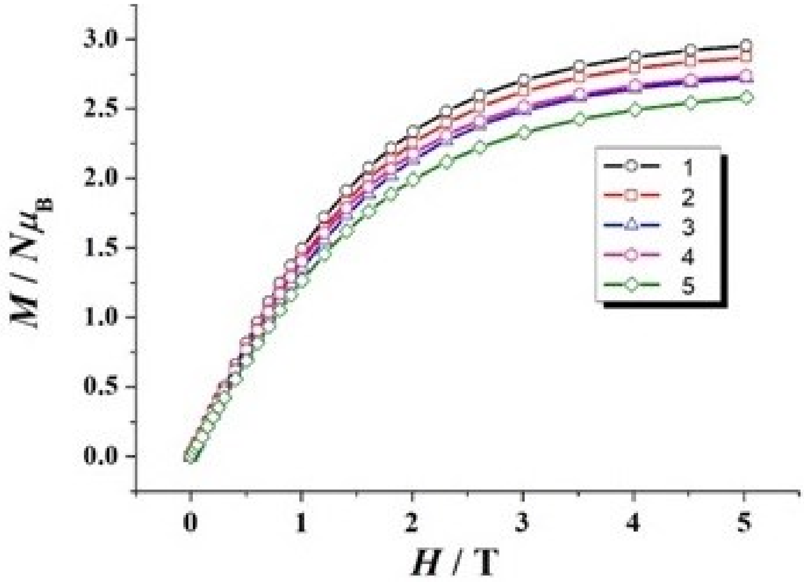

Fig. S6. Magnetisation plots of complexes **1−5**.

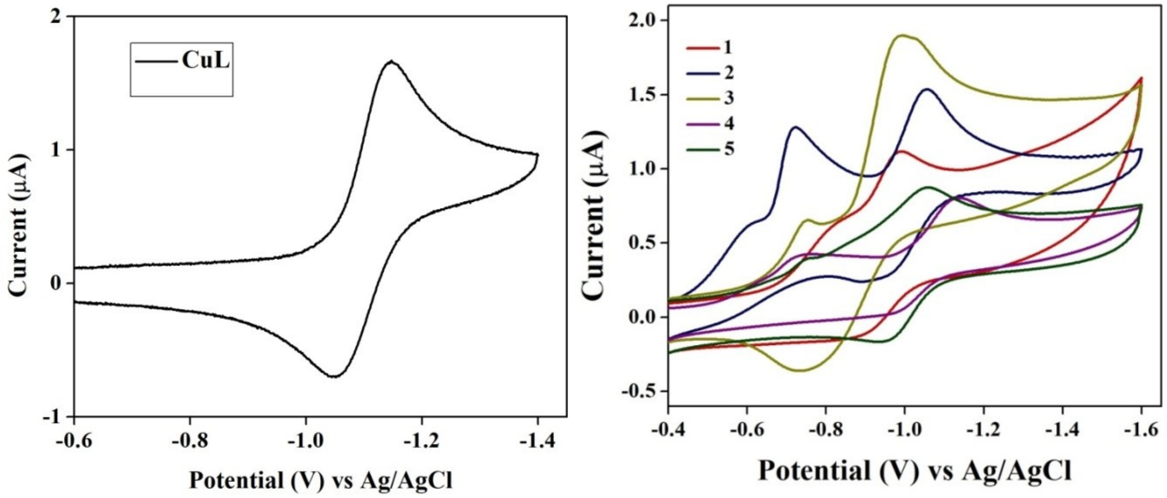

Fig. S7. Cyclic voltammograms (CVs) of 10^{-3} M solution of CuL (left) and complexes **1−5** (right) in acetonitrile at room temperature and a scan rate of 100 mV/Sec, using TBAP as supporting electrolyte.

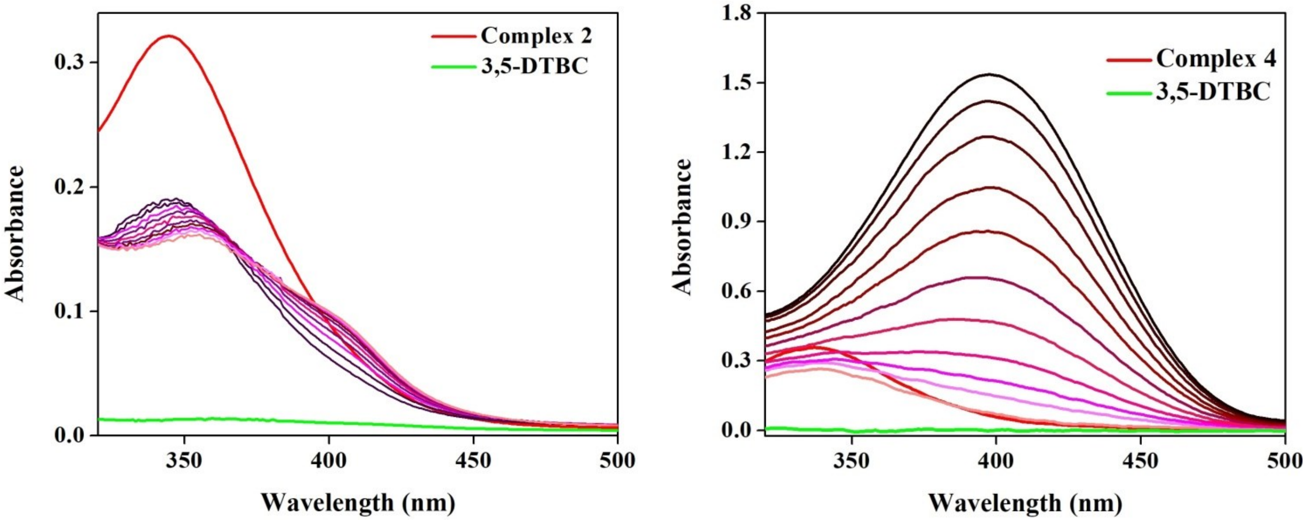

Fig. S8. Increase in the 3,5- DTBQ band at around 398 nm after adding equal volumes of 2 x 10^{-3} M of 3,5-DTBC to a 2 x 10^{-5} M acetonitrile solution of complexes **2** and **4**. The spectra were recorded at 3 min interval for 30 min.

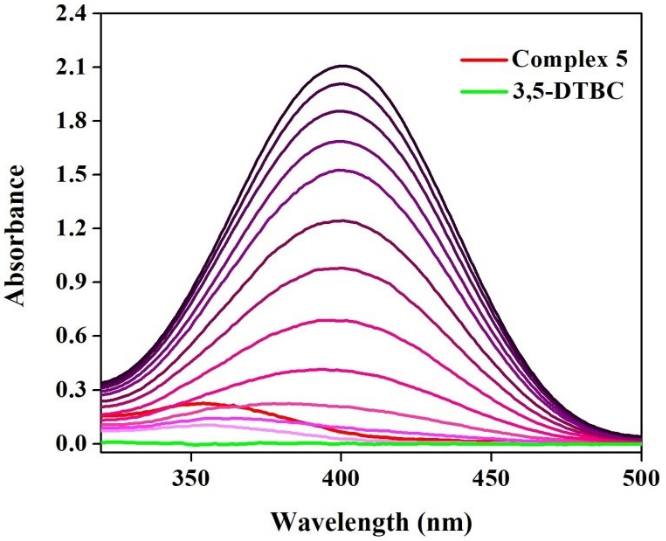

Fig. S9. Increase in the 3,5- DTBQ band at around 398 nm after adding equal volumes of 2 x 10^{-3} M 3,5-DTBC to a 2 x 10^{-5} M acetonitrile solution of complex **5**. The spectra were recorded at 3 min interval for half an hour.

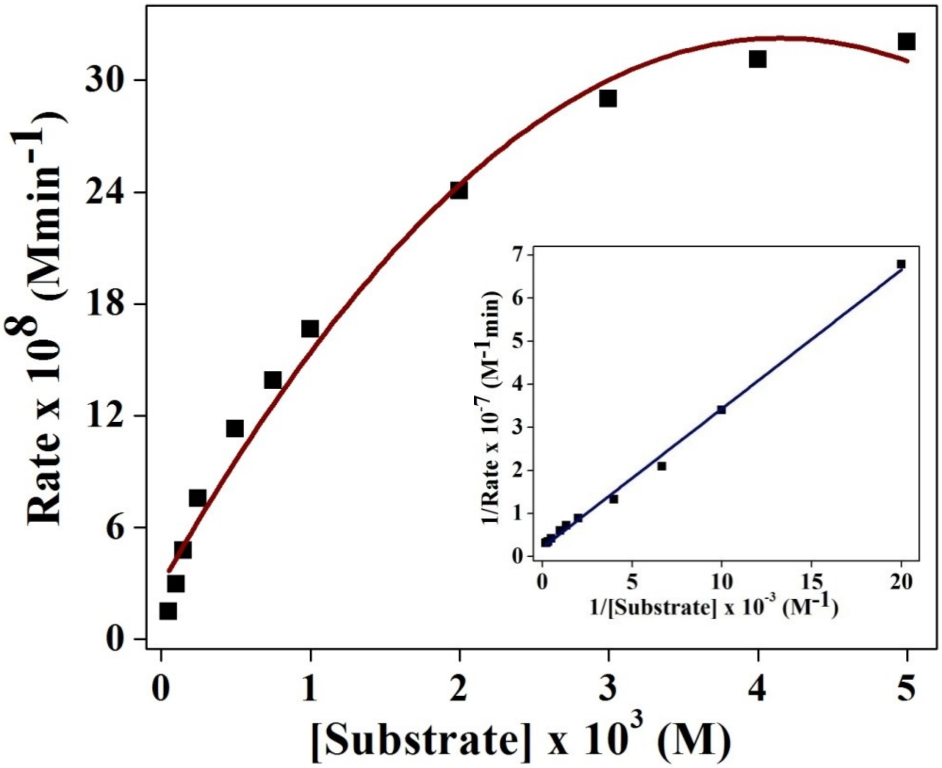

Fig. S10. Plots of rate *vs*. substrate concentration for complex **4**. The insets show the corresponding Lineweaver-Burk plot.

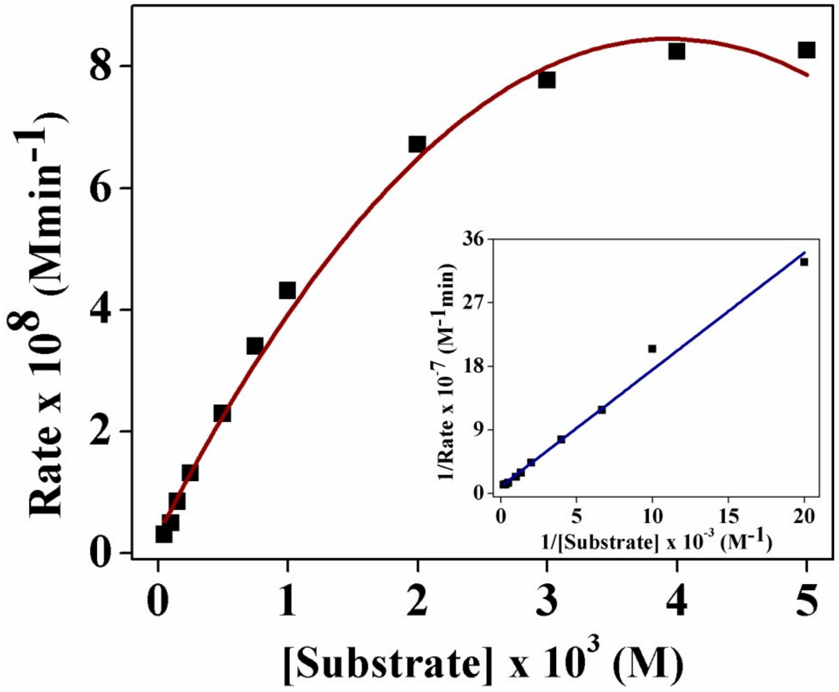

Fig. S11. Plots of rate *vs*. substrate concentration for complex **5**. The insets show the corresponding Lineweaver-Burk plot.

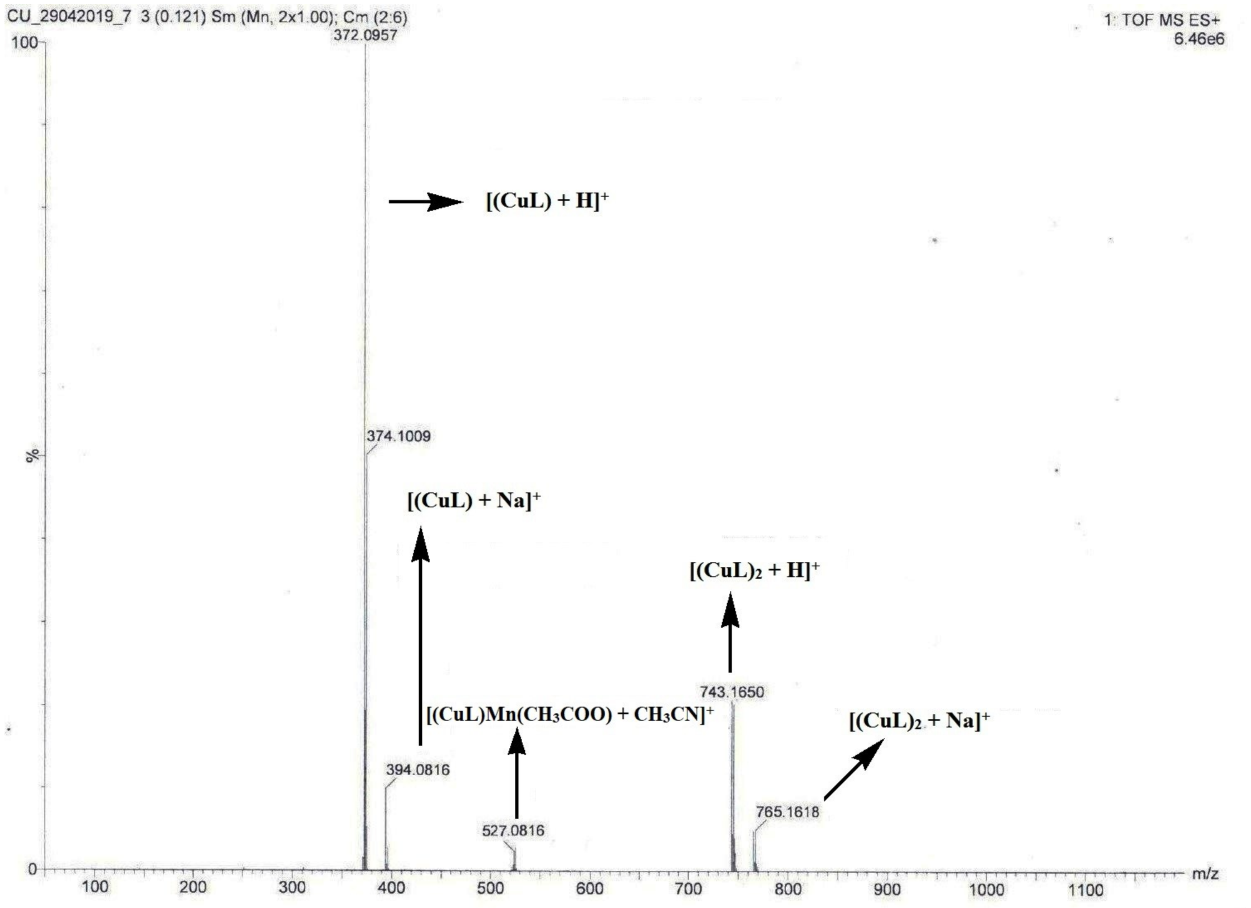

Fig. S12. Representative ESI mass spectrum of complex **1**.

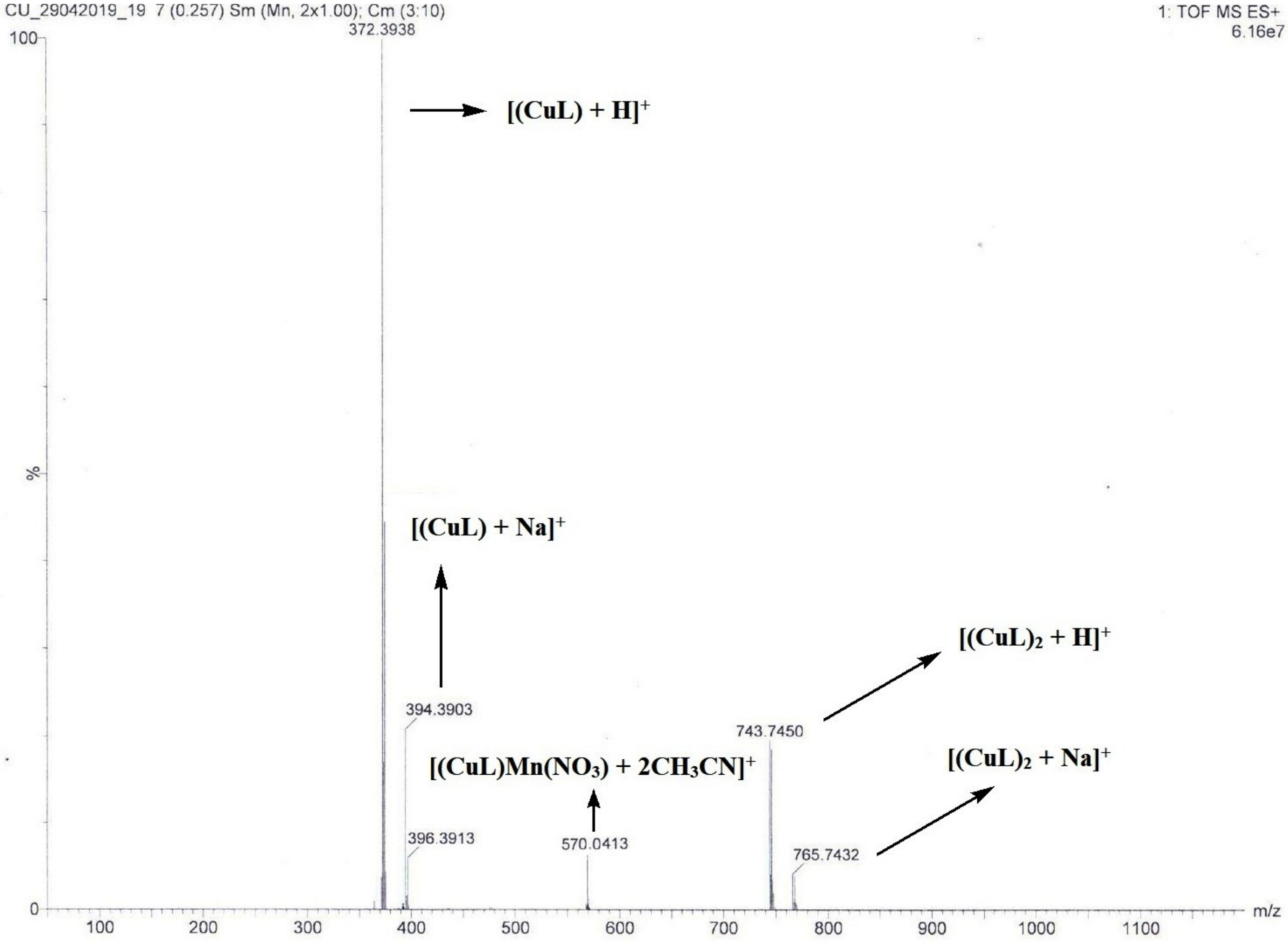

Fig. S13. Representative ESI mass spectrum of complex **2**.

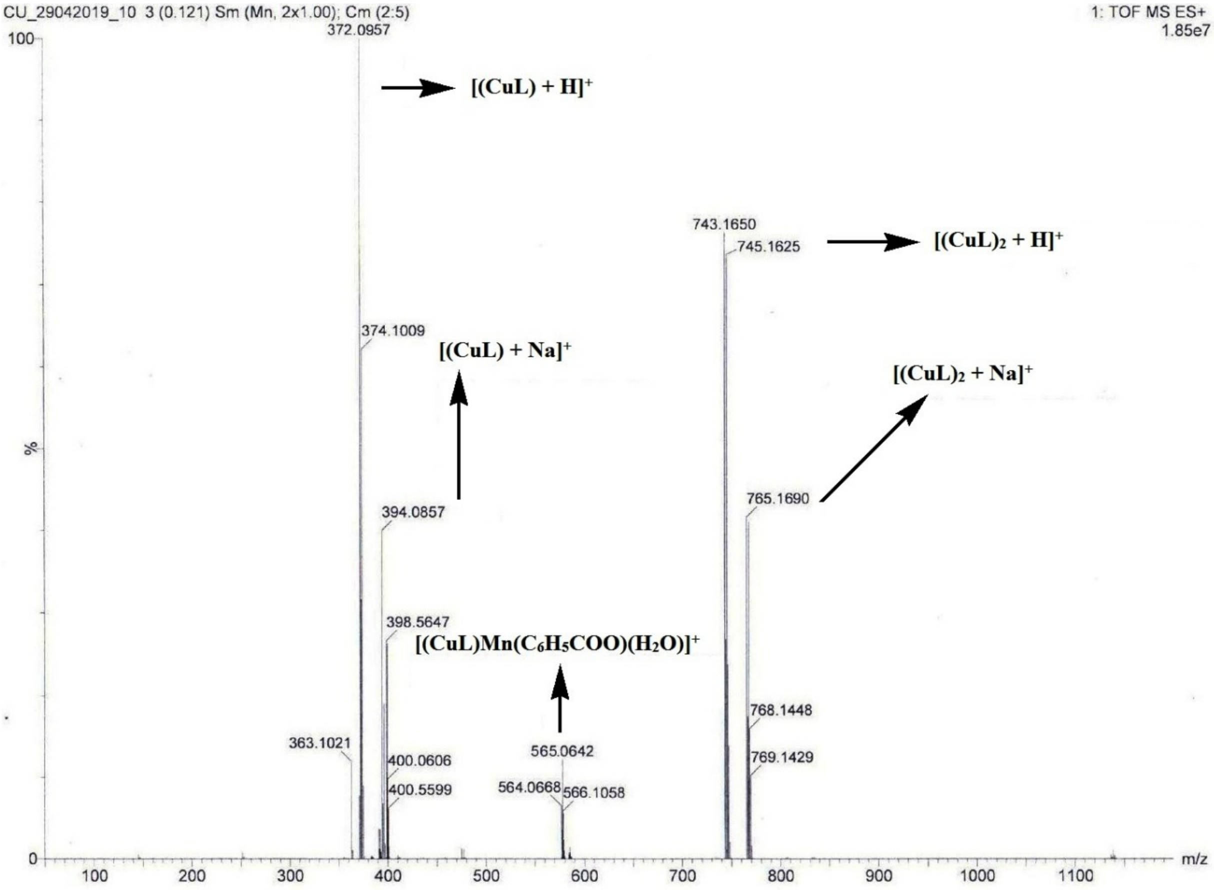

Fig. S14. Representative ESI mass spectrum of complex **3**.

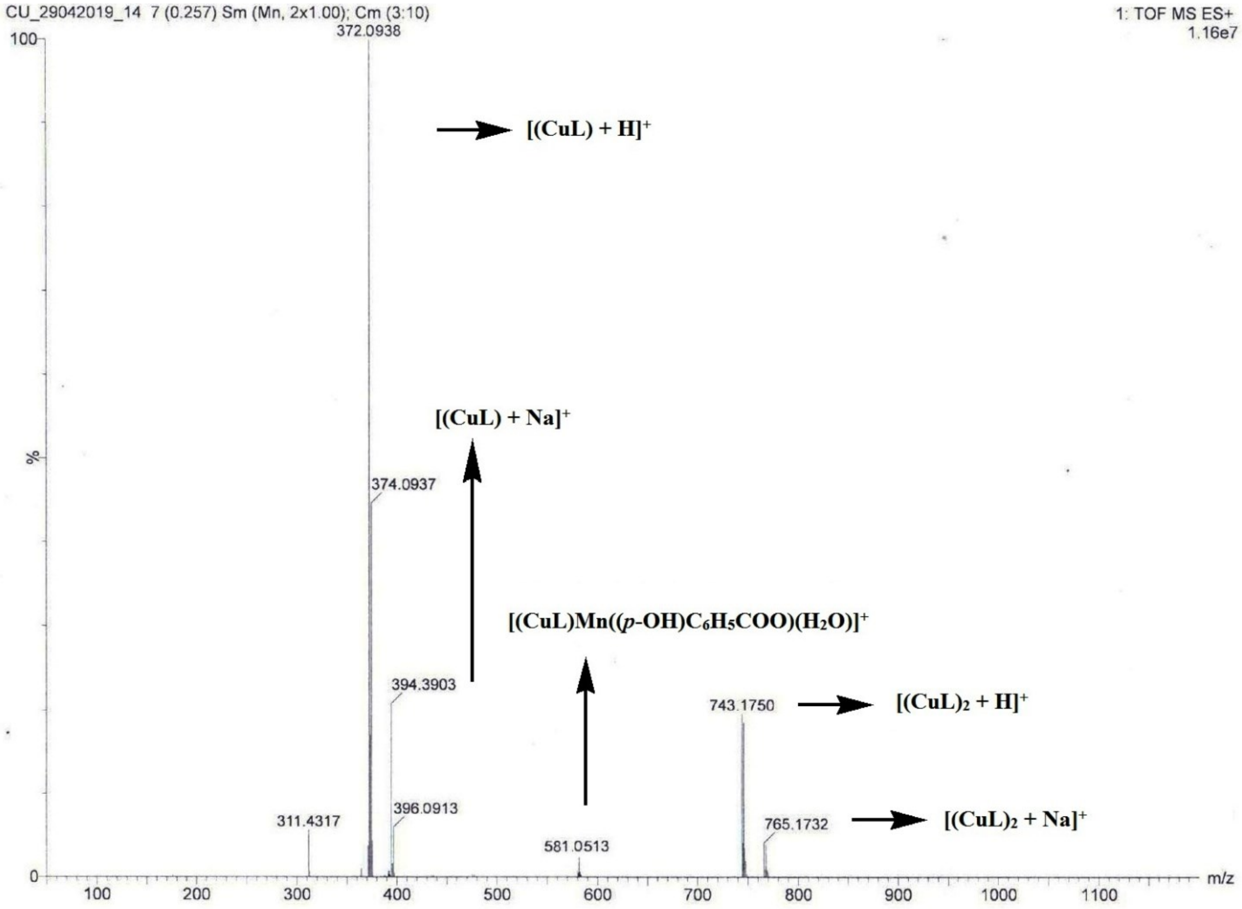

Fig. S15. Representative ESI mass spectrum of complex **4**.

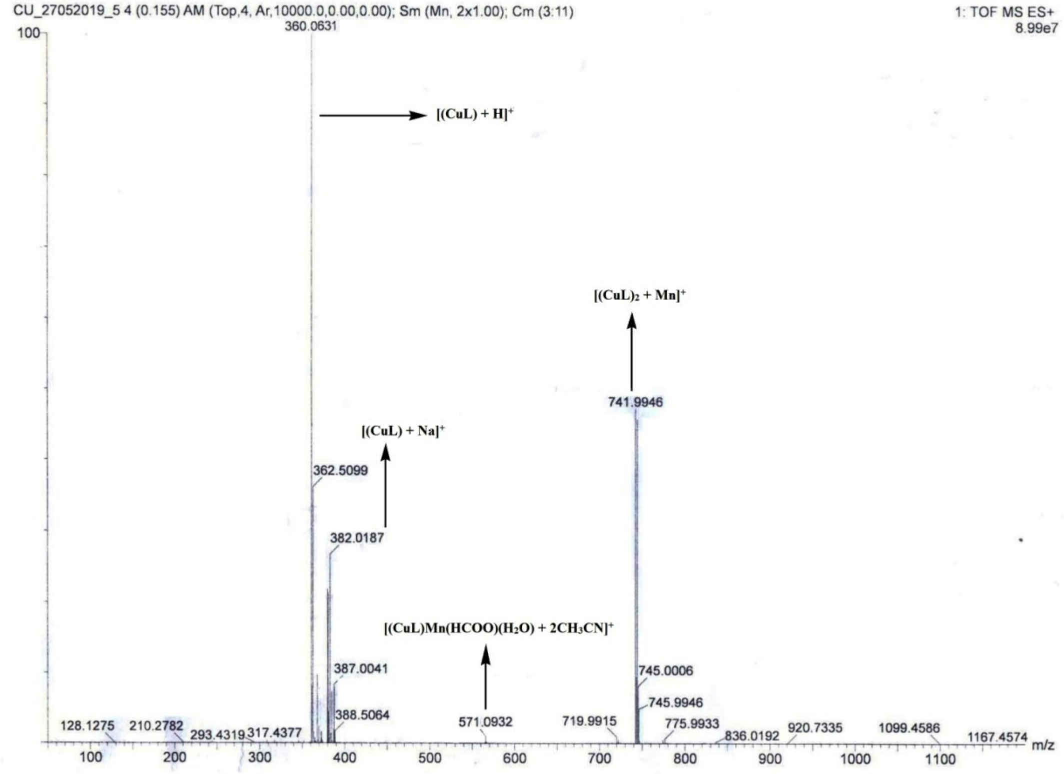

Fig. S16. Representative ESI mass spectrum of complex **5**.

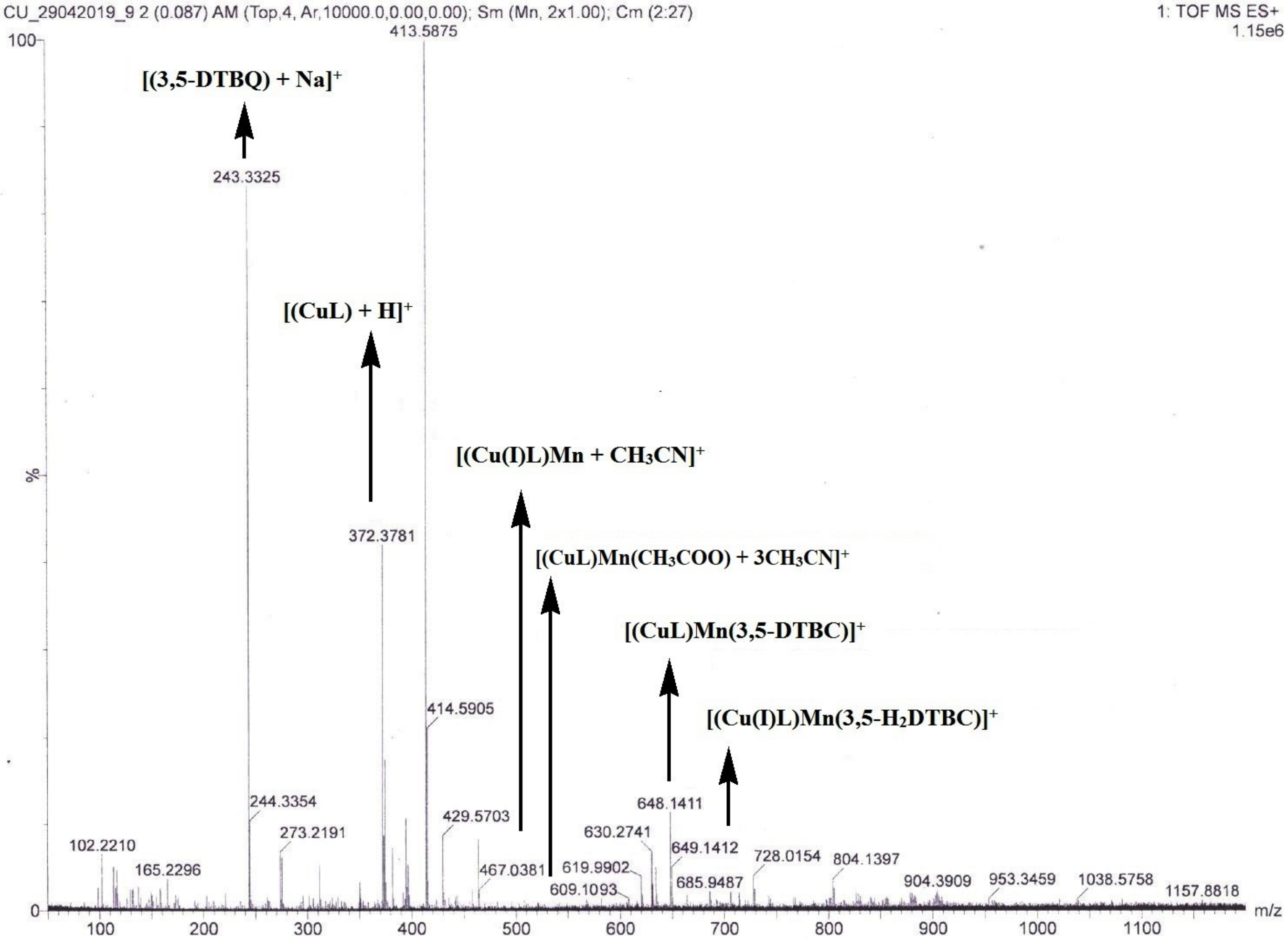

Fig. S17. Representative ESI mass spectrum of complex **1** with 3,5-DTBC.

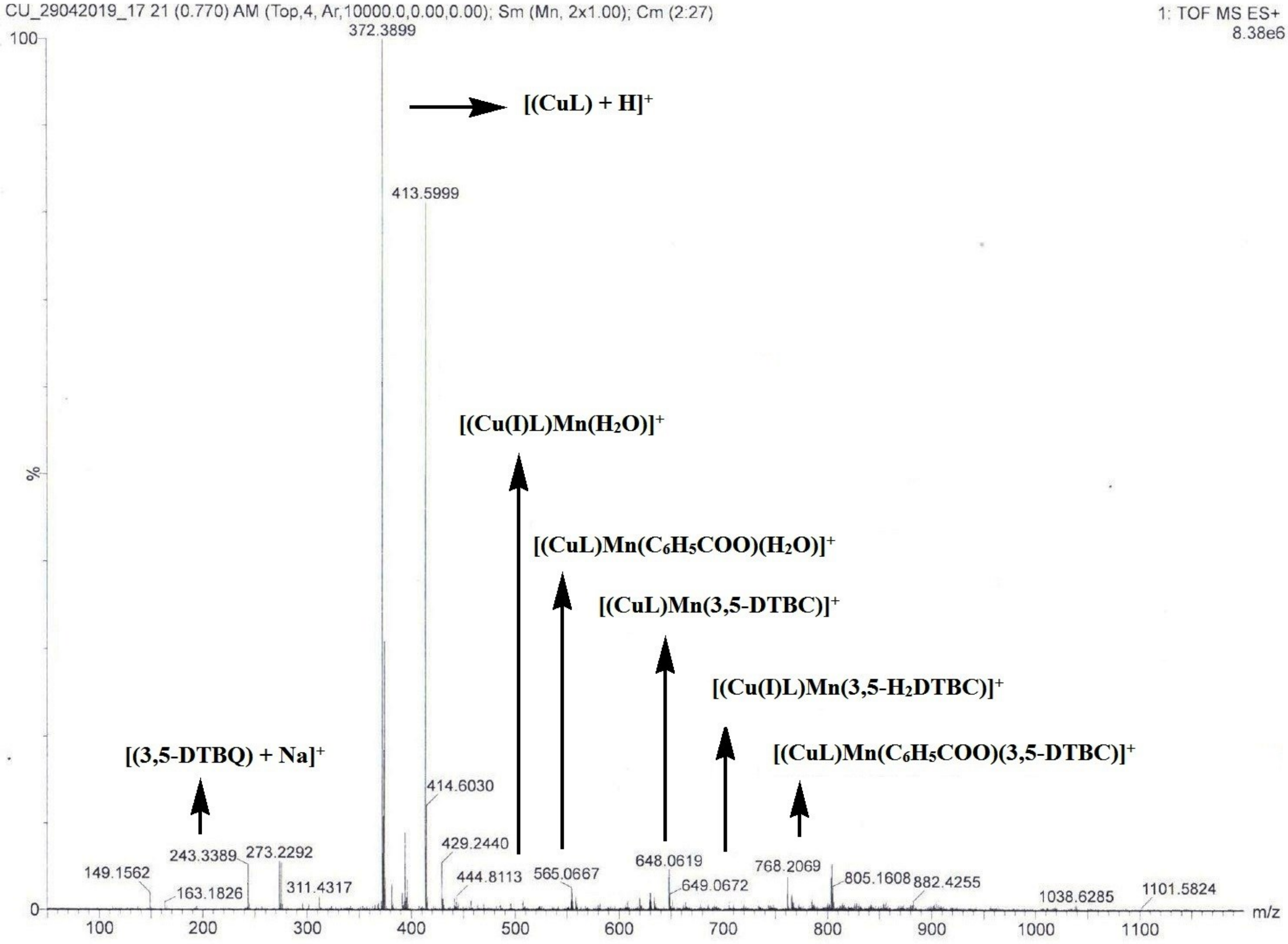

Fig. S18. Representative ESI mass spectrum of complex **3** with 3,5-DTBC.

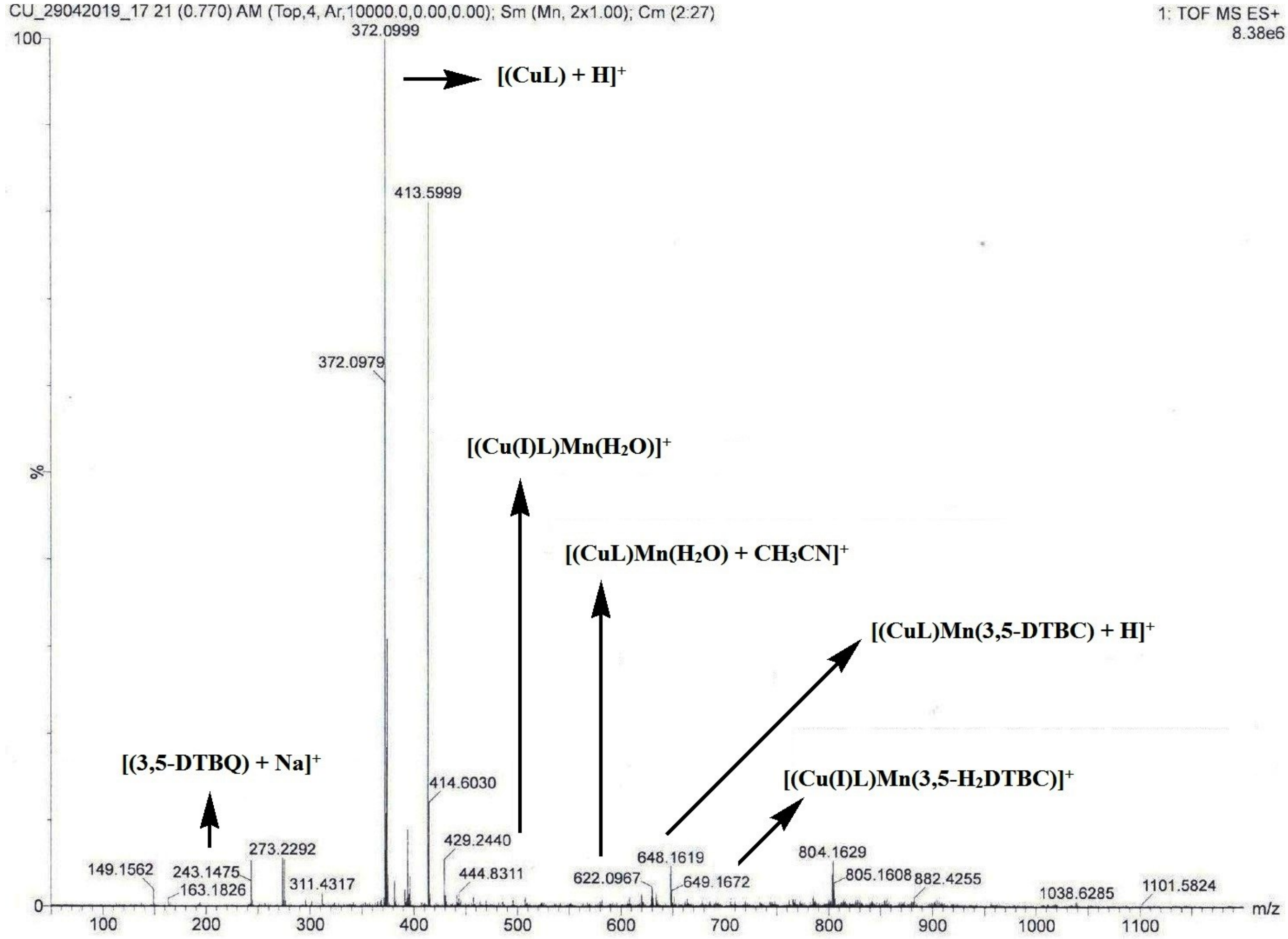

Fig. S19. Representative ESI mass spectrum of complex **4** with 3,5-DTBC.

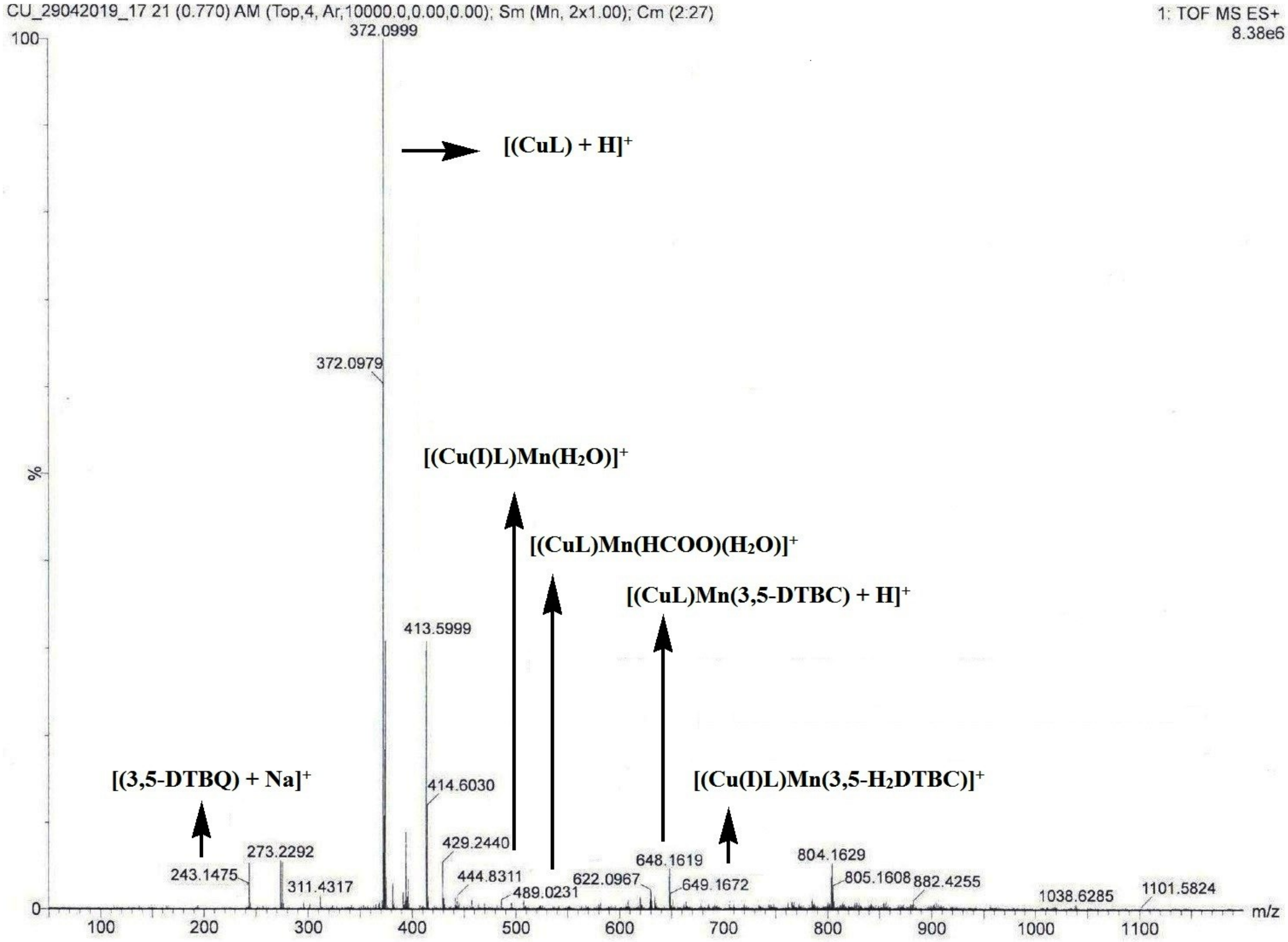

Fig. S20. Representative ESI mass spectrum of complex **5** with 3,5-DTBC.

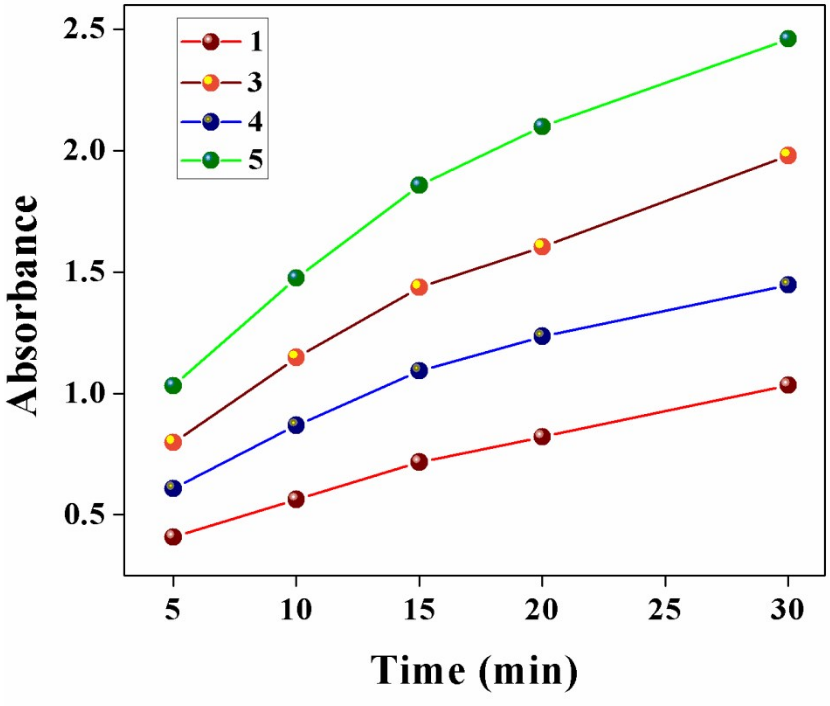

Fig. S21. Plot of H_2O_2 estimation of complexes **1–5**.

Complex and catechol solutions were prepared and mixed as needed for kinetic studies. After an hour, the pH of the solution was brought to 2 by acidifying it with H_2SO_4. Simultaneously an equal volume of water was added, to restrain any further oxidation. The quinone (3,5-DTBQ) formed as product was extracted thrice with dichloromethane. Furthermore, 1 mL of a 10% solution of KI and three drops of 3% solution of ammonium molybdate were added to the aqueous layer and formation of I^{3-} was monitored spectrophotometrically by growth of its characteristic absorption band at $\lambda = 353$ nm ($\varepsilon = 26000$ $M^{-1}cm^{-1}$).

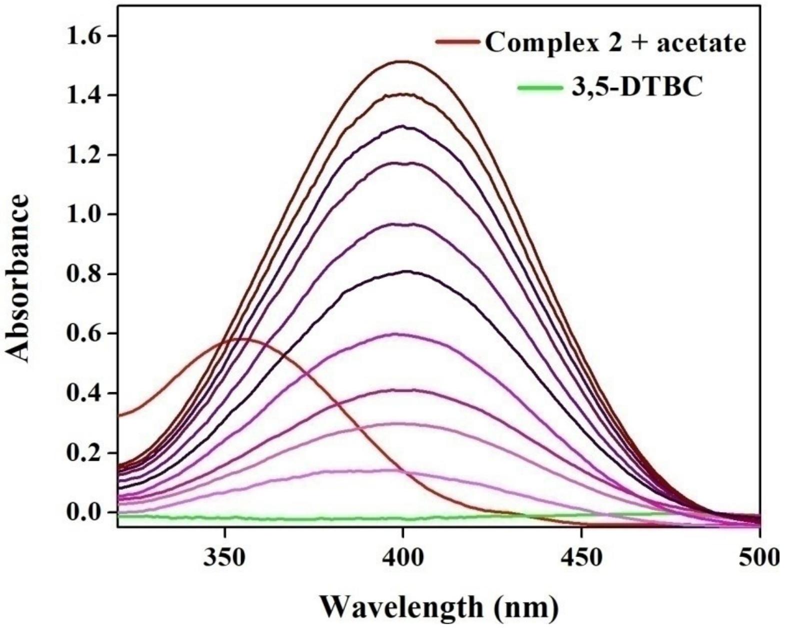

Fig. S22. Increase in the 3,5-DTBQ band at around 398 nm after adding equal volumes of 2×10^{-3} M 3,5-DTBC to an acetonitrile solution of complex **2** (2×10^{-5} M) + CH_3COONa (4×10^{-5} M). The spectra were recorded at 3 min interval for half an hour.

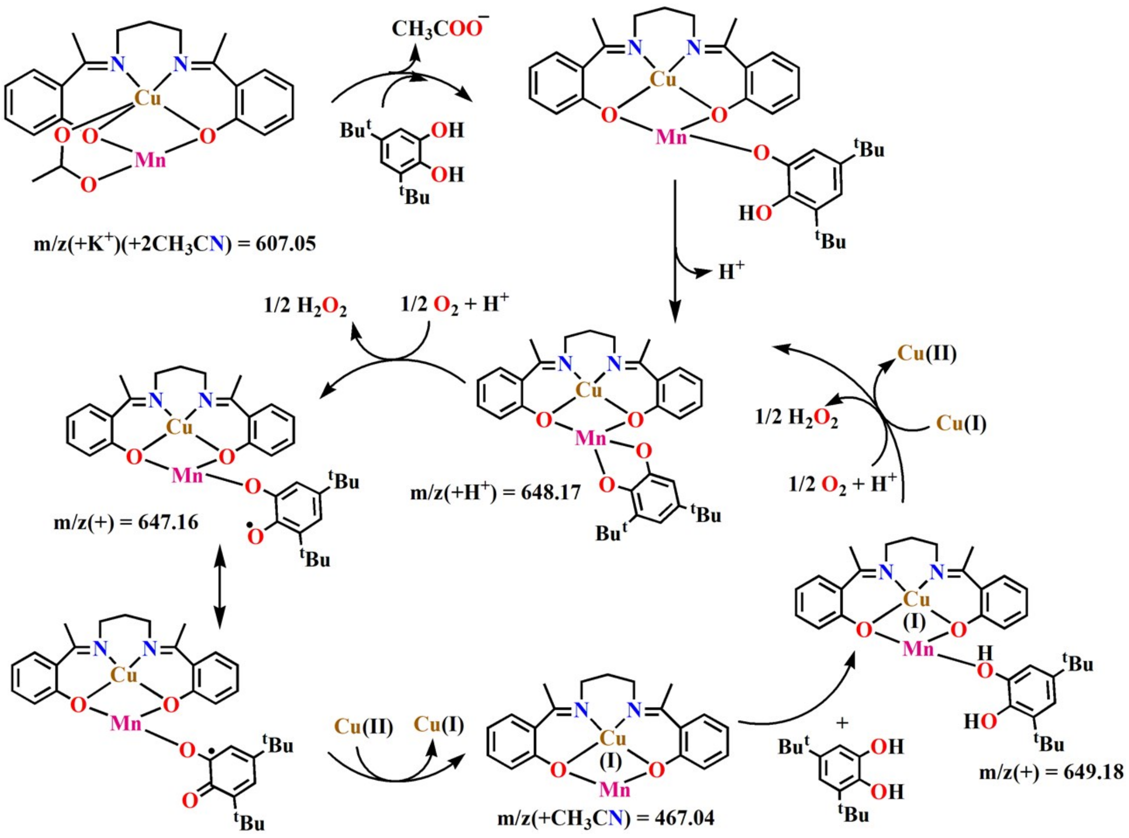

Scheme S1: Proposed Mechanism for Catalytic Oxidation of 3,5-DTBC to 3,5-DTBQ by Complex **1**.

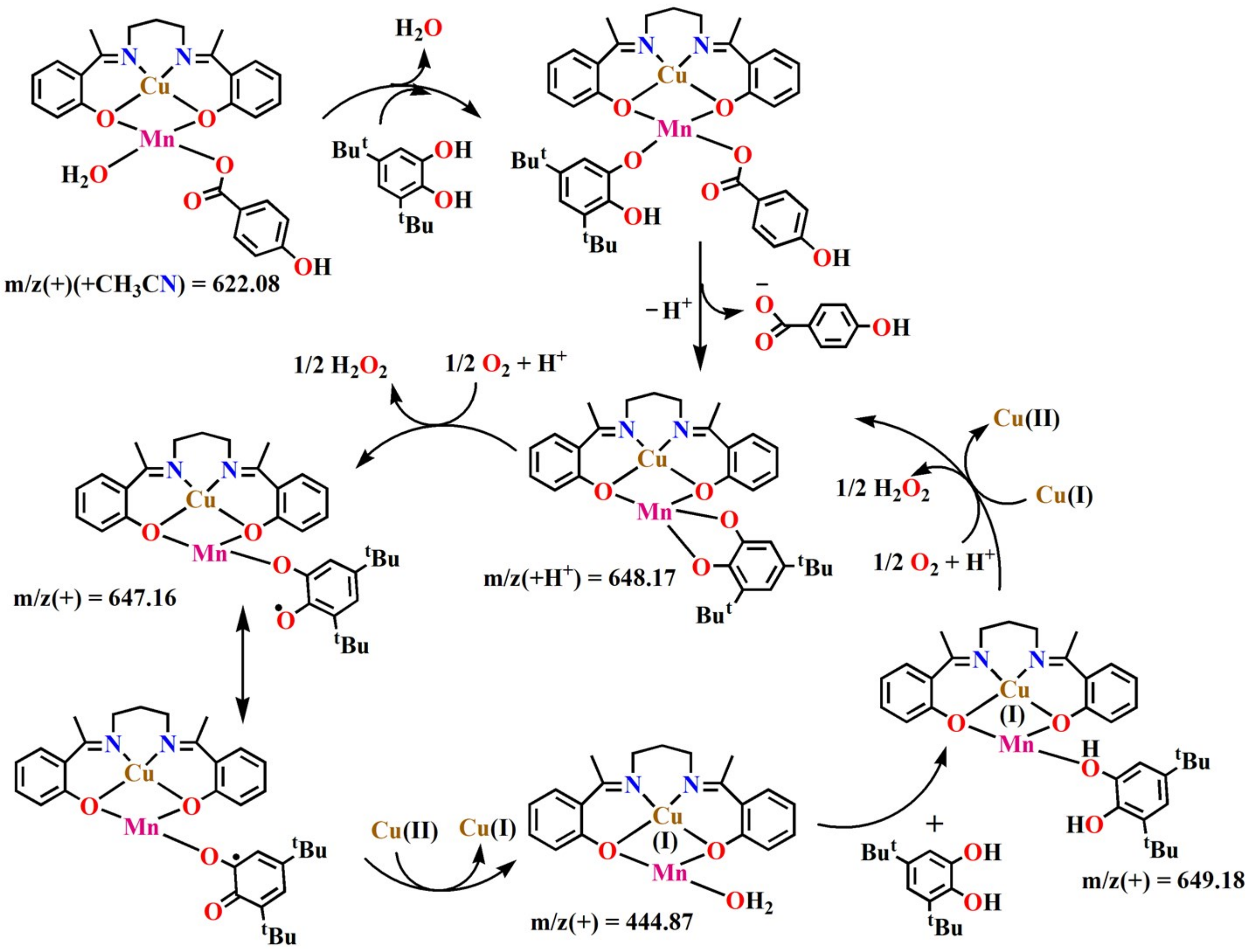

Scheme S2: Proposed Mechanism for Catalytic Oxidation of 3,5-DTBC to 3,5-DTBQ by Complex **4**.

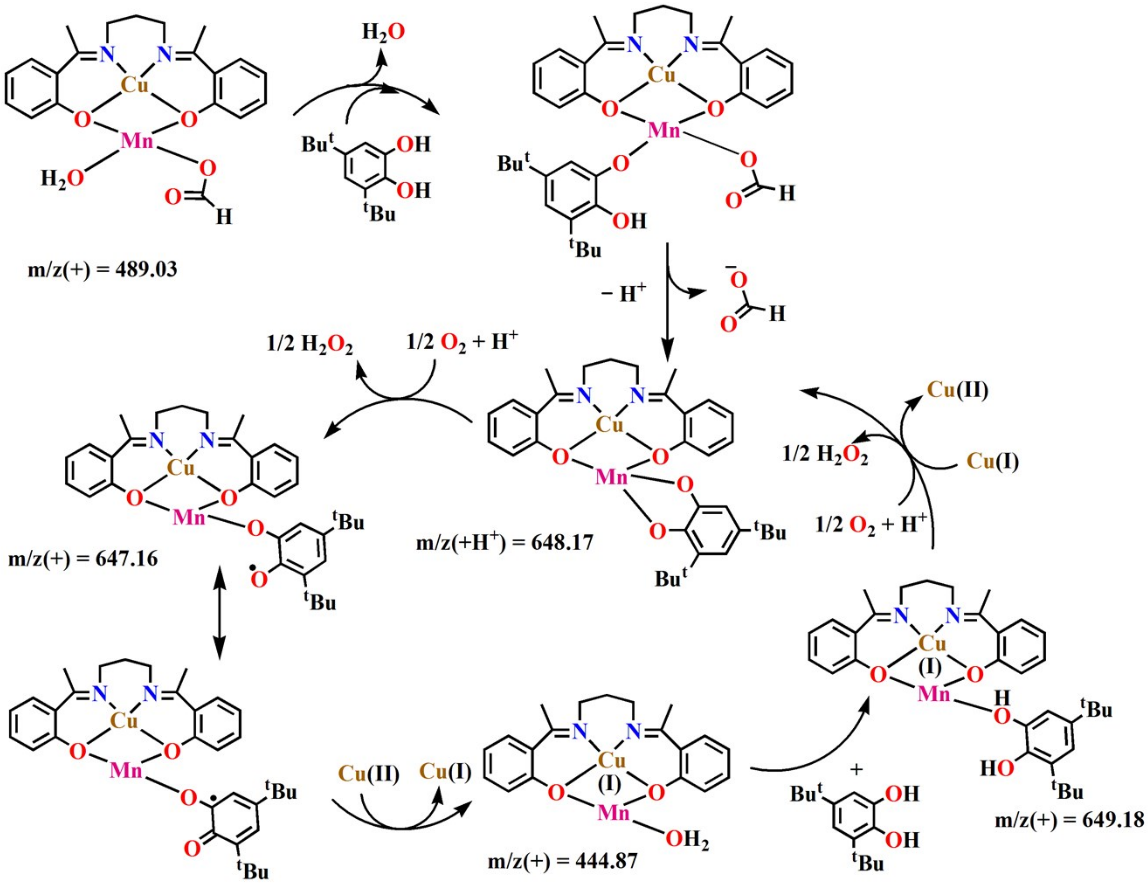

Scheme S3: Proposed Mechanism for Catalytic Oxidation of 3,5-DTBC to 3,5-DTBQ by Complex **5**.

Table S1. Dimensions (distances, (Å) & Angles (°)), in the metal coordination spheres of **1** and **2**

M–L	**1**	**2A**	**2B**
Cu(1)–O(11)	1.976(2)	1.955(4)	1.952(4)
Cu(1)–O(31)	1.924(2)	1.945(4)	1.947(4)
Cu(1)–N(19)	1.977(2)	1.970(5)	1.981(5)
Cu(1)–N(23)	2.001(2)	1.983(5)	1.983(5)
Cu(1)–O(41)	2.218(2)	2.418(5)	
Mn(1)–O(11)	2..195(2)	2.173(4)	2.171(4)
Mn(1)–O(31)	2.199(2)	2.186(4)	2.159(4)
Mn(1)–O(43)	2.127(2)	2.197(4)	2.192(5)

Cu(1)–Mn(1)	3.1151(4)	3.1193(7)	3.1200(6)
O(11)–Cu(1)–O(31)	83.96(7)	85.2(2)	84.6(2)
O(11)–Cu(1)–N(19)	87.98(8)	89.3(2)	89.5(2)
O(31)–Cu(1)–N(19)	169.13(8)	174.1(2)	170.5(2)
O(11)–Cu(1)–N(23)	160.35(8)	168.1(2)	173.8(2)
O(31)–Cu(1)–N(23)	90.19(8)	89.7(2)	89.8(2)
N(19)–Cu(1)–N(23)	95.03(9)	95.3(2)	95.9(2)
O(31)–Cu(1)–O(41)	92.34(7)	86.8(2)	
O(11)–Cu(1)–O(41)	96.18(7)	87.8(2)	
N(19)–Cu(1)–O(41)	95.78(8)	95.0(2)	
N(23)–Cu(1)–O(41)	102;80(8)	102.6(2)	
O(31)–Mn(1)–O(11)	72.83(6)	74.53(14)	74.57(14)
O(43)–Mn(1)–O(11)	87.01(7)	90.70(16)	88.65(17)
O(43)–Mn(1)–O(31)	91.23(7)	90.86(16)	88.40(17)

Table S2. Dimensions (distances, (Å) & Angles (°)) in the metal coordination spheres of **3**

M−L	
Cu(1)−O(11)	1.925(4)
Cu(1)−O(31)	1.909(4)
Cu(1)−N(19)	1.985(5)
Cu(1)−N(23)	1.949(5)
Mn(1)−O(41)	2.039(19)
Mn(1)−O(11)	2..109(4)
Mn(1)−O(1W)	2.209(17)
Mn(1)−O(31)	2.289(4)
Cu(1)−Mn(1)	3.1165(11)
O(11)−Cu(1)−O(31)	82.3(2)
O(11)−Cu(1)−N(19)	89.6(2)
O(31)−Cu(1)−N(19)	162.9(2)
O(11)−Cu(1)−N(23)	167.1(2)
O(31)−Cu(1)−N(23)	90.5(2)
N(19)−Cu(1)−N(23)	100.1(2)
O(41)−Mn(2)−O(11)$1	101.7(5)
O(41)−Mn(2)−O(11)	101.0(5)
O(11)−Mn(2)−O(11)$1	146.2(2)
O(11)−Mn(1)−O(1W)	112.9(5)
O(11)$1−Mn(1)−O(1W)	92.6(5)
O(41)−Mn(1)−O(31)$1	96.3(5)
O(11)−Mn(1)−O(31)$1	83.6(2)
O(11)−Mn(1)−O(31)	69.8(2)
O(41)−Mn(1)−O(31)	167.7(5)
O(1W)−Mn(1)−O(31)	104.5(5)
O(31)−Mn(1)−O(31)$1	74.9(3)

O(1W)−Mn(1)−O(31)$1	162.5(5)

Symmetry element $1 = 1 − *x*, *y*, 3/2 − *z*

Table S3. Selected Bond Lengths (Å) & Angles (°) of the disordered complexes **4** and **5**.

M−L	**4**	**5**
Cu(1)–O(11)	1.894(6)	1.914(6)
Cu(1)–O(31)	1.926(5)	1.938(6)
Cu(1)–N(19)	1.964(7)	1.945(7)
Cu(1)–N(23)	1.971(8)	1.974(8)
Cu(2)–O(41)	1.894(6)	1.901(7)
Cu(2)–O(61)	1.938(5)	1.924(6)
Cu(2)–N(49)	1.968(6)	1.946(8)
Cu(2)–N(53)	1.983(7)	1.998(10)
Mn(1)–O(71)	2.079(5)	2.108(7)
Mn(1)–O(61)	2.118(5)	2,114(6)
Mn(1)–O(31)	2.126(6)	2.119(6)
Mn(1)–O(1)	2.164(6)	2.183(7)
Mn(1)–O(41)	2.273(5)	2.234(6)
Mn(1)–O(11)	2.326(6)	2.346(6)
Cu(2)–Mn(1)	3.129(2)	3.110(2)
Cu(1)–Mn(1)	3.171(2)	3.142(2)
O(41)–Cu(2)–O(61)	81.4(2)	81.9(3)
O(41)–Cu(2)–N(49)	90.7(2)	91.5(3)
O(61)–Cu(2)–N(49)	171.5(3)	171.9(3)
O(41)–Cu(2)–N(53)	167.0(2)	167.5(3)
O(61)–Cu(2)–N(53)	87.3(3)	87.9(3)
N(49)–Cu(2)–N(53)	100.9(3)	99.2(4)
O(11)–Cu(1)–O(31)	81.0(2)	82.4(3)
O(11)–Cu(1)–N(19)	91.6(2)	91.3(3)
O(31)–Cu(1)–N(19)	170.7(3)	170.4(3)

O(11)–Cu(1)–N(23)	166.7(2)	164.8(3)
O(31)–Cu(1)–N(23)	88.1(3)	88.3(3)
N(19)–Cu(1)–N(23)	99.9(3)	99.3(3)
O(71)–Mn(1)–O(61)	106.8(2)	110.0(3)
O(71)–Mn(1)–O(31)	93.9(2)	92.7(3)
O(61)–Mn(1)–O(31)	150.4(2)	151.2(2)
O(71)–Mn(1)–O(1)	89.2(2)	87.7(2)
O(61)–Mn(1)–O(1)	96.4(2)	94.4(3)
O(31)–Mn(1)–O(1)	104.8(2)	104.3(3)
O(71)–Mn(1)–O(41)	95.4(2)	94.7(3)
O(61)–Mn(1)–O(41)	69.2(2)	70.4(3)
O(31)–Mn(1) − O(41)	88.4(2)	91.0(2)
O(1)–Mn(1)–O(41)	165.7(2)	164.5(3)
O(71)–Mn(1)–O(11)	160.3(2)	159.8(3)
O(61)–Mn(1)–O(11)	88.4(2)	85.2(2)
O(31)–Mn(1)–O(11)	67.6(2)	69.1(2)
O(1)–Mn(1)−O(11)	101.6(2)	104.9(2)
O(41)−Mn(1)−O(11)	78.0(2)	77.4(2)
Cu(1)−Mn(1)−Cu(2)	80.8(1)	81.30(3)

Table S4: Geometrical features of hydrogen bonding interactions (distances (Å) and angles(°)) of Complex **2**.

D−H···A	D−H	H···A	D···A	∠D−H···A
O(1)–H(1)…O(44A)[a]	0.82	2.39(2)	2.806(13)	112
O(1)–H(1)…O(2)	0.82	1.93	2.62(2)	142
O(2)–H(2)…O(1)	0.80	1.84	2.62(2)	166

where [a] = $x, -1 + y, z$

Table S5: Geometrical features of hydrogen bonding interactions (distances (Å) and angles(°)) of Complex **4**.

D−H···A	D−H	H···A	D···A	∠D−H···A
O(1W)–H(1W)…O(73)	0.85(2)	1.87(6)	2.622(8)	146(9)
O(1W)–H(2W)…O(7W)	0.84(2)	2.04(10)	2.752(14)	142(15)
O(1W)–H(2W)…O(6W)	0.84(2)	1.94(5)	2,75(3)	161(10)

Table S6: Geometrical features of hydrogen bonding interactions (distances (Å) and angles(°)) of Complex **5**.

D−H···A	D−H	H···A	D···A	∠D−H···A
O(1)–H(1)…O(73)	0.85	1.81	2.626(10)	159
O(91)–H(91)…O(1)	0.90	1.70	2.587(17)	170

Table S7: *J* parameter for all the reported complexes with a double phenoxo bridge according to the Spin-Hamiltonian $H = -2J \cdot S_1 S_2$, (α + β)/2 and the torsion angle M(II)−O−Cu(II)−O.

CCDC name	***J*/cm^{-1}**	**(α + β)/2/deg**	**M(II)−O−Cu(II)−O torsion/deg**
BICBIA	-15.9	102.66	9.01
BICCAT	-29.1	106.89	6.14
CEPPUL	-35.77	106.32	2.50
CEPPLIT	-24.2	105.04	12.47
CEPPOF	-22.77	103.45	10.29
CEPQAS	-19.83	100.19	2.42
DEXQUIT	-17.4	103.75	0.00

FAEPCU	-13.2	95.7	26.05
GAJXUM	-35.80	107.5	0.88
ILAKOV	-11.0	101.6	13.22
LEGJAI	-22.4	100.2	12.01
MIXLEL	-15.9	103.42	3.46
QEKFIW	-18.4	100.90	9.89
UNIPEJ	-30.0	100.47	8.52
VOBLAA	-48.9	105.98	3.42
YUVRAJ	-15.1	103.75	2.40
AGSD1	-13.5	101.5	6.2
AGSD2	-13.5	101.85	2.71
AGSD3	-12.6	102.32	3.63
AGSD4	-13.24	102.08	8.82
1	-8.54	97.16	23.32
2	-11.50	98.32	16.51
3	-19.83	98.40	25.11
4	-10.65	98.21	15.06
5	-10.27	98.30	17.90